

Investigation of Fracture Formation During Bending of 5xxx Series Aluminum Alloys

Mehmet Okan Görtan^{1*} , Mehmet Ali Çiftçi^{1,2} 

¹Department of Mechanical Engineering, Hacettepe University, Ankara / Türkiye

²FNSS Defense Industries, Ankara / Türkiye

Keywords

Aluminum sheets,
EN AW 5083 alloy,
V-bending,
Fracture formation,
Finite element
analysis.

Abstract

Aluminum alloys are frequently used in the defense industry thanks to their lightweight and comparatively high strength. In the current study, bending and fracture formation characteristics of EN AW 5083-H321 aluminum sheets are investigated using bending tests and finite element analysis. Bending tests are conducted using three different thicknesses in sheet metals, namely 3 mm, 4 mm, and 6 mm. Furthermore, five different bending radii is combined with those thicknesses. Limiting bending radius to thickness ratios are determined using experiments. Those experiments are modeled using finite element analysis. Consequently, fracture parameters of the investigated material are defined to be able to accurately model the process. Therefore, a valuable tool has been developed to aid designers in future applications.

1. Introduction

Aluminum alloys are commonly utilized in the defense sector due to their favorable strength-to-weight ratio, ease of forming, and outstanding resistance to corrosion [1–3]. These materials typically undergo various shaping techniques to achieve their final form, with bending being one of the primary methods used to shape them as required. In its general form, bending is described as the forming process to generate a curvature in parts using a moment applied around the longitudinal axis of the metals. As a results of curvature generation, outside of the bent parts stretched and inside is compressed [4]. The major failure mechanism especially in the stretched outside of the bent sections is fracture formation. The allowable bending angle and radius are significantly influenced by factors such as the part's size and thickness, the material's properties, and the die design. These elements directly impact the resulting strain values [5].

In the current study, bending and fracture formation characteristics of EN AW 5083-H321 aluminum alloy have been investigated using bending tests and finite element analysis. In existing systems, the bending process is carried out based on outdated standards. Designers choose the bending angle and radius according to specified thickness ranges defined in these standards. The key contribution of this study is its approach to determining a unique bending radius for each specific thickness, rather than relying on predefined intervals. Materials with three different thicknesses are used. All samples are bent using V-bending in a CNC press. Fracture formation on the outside of the bent samples are investigated using liquid penetrant tests. Additionally, a finite element model of the bending process was developed using MSC.Marc 2022.2 software. Finite element results are compared and validated with the test results.

* Corresponding Author: okangortan@hacettepe.edu.tr

Received: April 16, 2025, Accepted: April 27, 2025

2. Materials and Methodology

In the current study, aluminum sheets made of EN AW 5083-H321 alloy has been used. The mechanical properties of the alloy were identified through tensile testing performed in accordance with the ASTM E8/E8M standard [5]. Three tests were carried out using a Zwick/Roell servo-hydraulic testing machine, and the average results are presented in Table 1.

Table 1. Mechanical properties of EN AW 5083-H321 alloy

Yield Strength [MPa]	Tensile Strength [MPa]	Elongation at Fracture [%]
238.7	373.1	24

Chemical composition of the material is taken from the supplier tests and is given Table 2. According to the supplier reports, this particular alloy is within the standard limits.

Table 2. Chemical composition of EN AW 5083-H321 alloy (in % wt)

Si	Fe	Cu	Mn	Mg	Cr	Zn	Ti	Al
0.38	0.35	0.06	0.78	4.45	0.09	0.21	0.08	bal.

The bending behavior of the aluminum alloys was examined in compliance with the ISO 7438:2020 standard. Samples with a width of 50 mm and length of 120 mm are prepared using laser cutting. Three different thicknesses have been investigated, namely 3 mm, 4 mm, and 6 mm. Furthermore, 5 different V-bending tools with different bending radii are manufactured. All samples are bent to 90° angle. An important characteristic of the bending process which affects stresses and strain in the materials is the bending radius to sheet thickness ratio [6]. Therefore, for each sheet thickness, different tools are used. Used bending matrix is represented in Table 3.

Table 3. Used bending matrix

Sheet Thickness	Bending Radius				
	3 mm	4 mm	6 mm	8 mm	12 mm
3 mm	X	X	X		
4 mm		X	X	X	X
6 mm		X	X	X	X

Based on the investigation matrix shown in Table 3, the ratio between bending radius to sheet thickness is calculated and represented in Table 4. Furthermore, for each of the investigated cases, engineering strain values are calculated using the Equation 1. In this equation, z is the distance between the middle of the sheet and the surface and r is the bending radius. Calculated engineering strain values are given in Table 5.

$$e = z/r \quad (1)$$

Table 4. Calculated bending radius to sheet thickness ratio of investigated cases

Sheet Thickness	Bending Radius				
	3 mm	4 mm	6 mm	8 mm	12 mm
3 mm	1.00	1.33	2.00		
4 mm		1.00	1.50	2.00	3.00
6 mm		0.66	1.00	1.33	2.00

Table 5. Calculated engineering strain values of investigated cases

Sheet Thickness	Bending Radius				
	3 mm	4 mm	6 mm	8 mm	12 mm
3 mm	0.500	0.375	0.250		
4 mm			0.333	0.250	0.166
6 mm		0.750	0.500	0.375	0.250

The bending operation was carried out using a TruBend 5230 hydraulic press, which has a capacity of 2300 kN and is equipped with a CNC unit. For all tests, the punch speed was consistently maintained at 15 mm/sec. To avoid any damage or deformation of the tooling, dies made from material with a hardness of 60 HRC were used. An image of the bending setup is provided in Figure 1.

**Figure 1.** Used bending press

To simulate crack formation during the bending of 5xxx series aluminum alloys, a finite element model of the process was developed using MSC.Marc 2022.2 software. Leveraging the symmetry of the setup, only half of the process was modeled. The sheet metal samples were defined as deformable bodies using fully integrated first-order quadrilateral elements, each with an edge length of 0.1 mm. The die and punch were treated as rigid bodies, with the die remaining stationary and the punch movement controlled via a displacement table.

Several strain hardening models have been proposed to describe the evolution of flow stress with plastic strain in metallic materials. Among these, the Hollomon model is widely used due to its simplicity, representing the stress-strain relationship through a power-law expression [7]. The Ludwik model extends the Hollomon formulation by incorporating a yield offset, providing a more accurate description for some metals [8]. The Swift model includes an initial strain parameter, making it particularly suitable for pre-strained materials [9]. Despite the utility of these models in various applications, they often fall short in accurately capturing the saturation behavior observed in aluminum alloys. In this study, the Voce model represented in Equation 2 is adopted, as it has been shown to effectively represent the asymptotic stress response of aluminum during plastic deformation, making it a suitable choice for analyzing strain localization and crack formation in bent aluminum sheets [10].

$$\sigma_{\text{true}} = \text{UTS} (1 - e^{-K(\epsilon + c)}) \quad (2)$$

In this equation, UTS is the ultimate tensile strength, K and c are material parameters. By fitting these two values to the tensile test results, material model is generated. Comparison of the tensile test results and derived material model is shown in Figure 2. Furthermore, the elastic modulus and Poisson's ratio are taken as 70 GPa and 0.33, respectively.

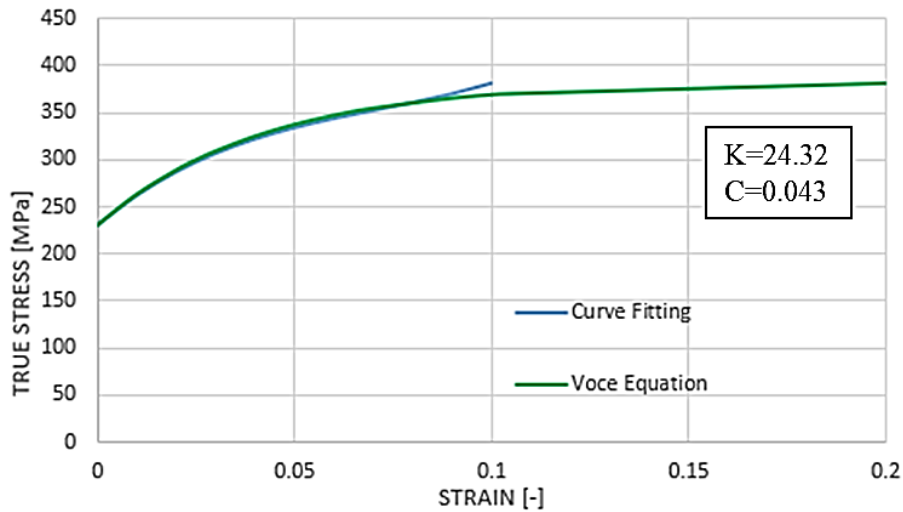


Figure 2. Comparison of the tensile test results and derived material model (Blue line is the test results)

In Figure 2, blue line indicates the true strain and true stress values obtained from tensile tests. It is obvious that tested aluminum material experiences a significant amount of strain hardening. However, after a certain strain level, in the current case 0.1, the strength of the material reaches saturation and stays nearly constant. In other words, the strength of the material doesn't grow with increasing strain anymore. Such mechanical material behavior is accurately modelled with Voce strain hardening law indicated with the green line in Figure 2. This model represents the stresses of the investigated material almost identically till a strain value of 0.1. For higher strain levels, strength of the material remains almost constant.

Various fracture models have been developed to predict the onset of damage and fracture in ductile materials under different loading conditions. These models generally fall into two categories: stress-based and strain-based criteria. The maximum principal stress criterion and the Mohr-Coulomb model are examples of stress-based approaches, often used for brittle materials or when fracture is driven by tensile stress peaks [11]. Strain-based models, such as the Johnson-Cook and Gurson-Tvergaard-Needleman (GTN) models [12, 13], incorporate plastic strain and void nucleation mechanisms to simulate ductile fracture processes more accurately. Among the widely used ductile fracture criteria, the Cockcroft-Latham damage model stands out for its simplicity and effectiveness, particularly in forming simulations [14-16]. It considers the accumulation of damage as a function of the maximum principal stress integrated over the plastic strain path, making it well-suited for predicting crack initiation in metal forming operations such as bending. In this study, the Cockcroft-Latham model presented with Equation 3 is employed to assess fracture initiation in aluminum sheets, due to its proven accuracy in capturing ductile fracture behavior under complex stress states.

$$\int_0^{\bar{\epsilon}_f} \sigma_{\max} d\bar{\epsilon} = c_1 \quad (3)$$

In this equation, σ_{\max} denotes the maximum principal stress, $\bar{\epsilon}$ represents the equivalent strain, $\bar{\epsilon}_f$ is the equivalent strain at the point of fracture, C_1 is a material constant that defines the threshold for ductile damage.

A representative sketch of the generated finite element model is shown in Figure 3 together with the applied boundary conditions.

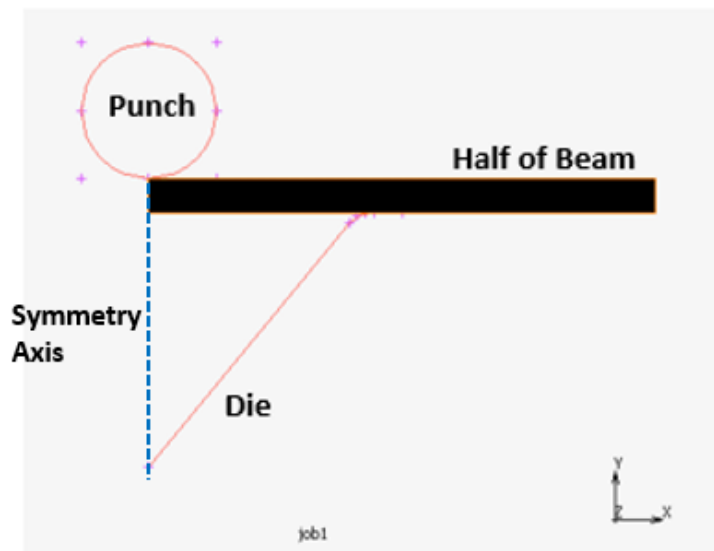


Figure 3. Finite element model of the bending process

3. Results and Discussion

In the first step of the investigations, a crack has been deliberately generated in all sheet thicknesses by bending. Therefore, samples with different sheet thicknesses are bent using a die with a 4 mm bending radius. Using iterative bending tests, the exact bending angle where the first crack is observed on the outer surface of the test samples is determined. Crack initiation angles for 3 mm, 4 mm, and 6 mm sheet thicknesses are 112°, 115°, and 138°, respectively. Afterwards, finite element simulations of the same bending processes are built. In those finite element simulations, bending is stopped exactly at the bending angle where crack started to initiate in the trials. Furthermore, the crack formation is also observed in the analysis. After iterative trials, it is observed that fracture formation can be exactly modeled when the $C1$ parameter in the Cockroft - Latham damage model is taken as 0.25. Furthermore, limit strain where the elements are erased are taken as 0.27. While using these parameters, the first element deleting is observed when the final bending for each sheet thickness is reached. Results of the bending tests and corresponding finite element simulations are shown in Figure 4.

After the fracture formation parameters are determined, iterative bending test have been conducted. All the bending variations in the Table 3 are investigated. Based on the DIN EN 00485-2 standard, each aluminum component has a specific minimum bending radius that varies depending on its series, temper condition, and thickness [17]. In line with the objectives of this study—to compare with standard values and determine the actual minimum bending radius—the selected aluminum samples were bent to 90° using various bending radii. Test results and corresponding finite element simulations where fractured and non-fractured samples with sheet thicknesses of 3 mm, 4 mm, and 6 mm are shown in Figure 5, Figure 6, and Figure 7, respectively.

The data implies that the damage parameters of Cockroft-Latham can show a realistic situation of material after bending activities. According to DIN EN 00485-2, the minimum aluminum bending radius in EN AW 5083 - H321 is given below [18]:

- 3 mm thickness sheet – 7.5 mm minimum bending radius
- 4 mm thickness sheet – 10.0 mm minimum bending radius
- 6 mm thickness sheet – 24.0 mm minimum bending radius

Nevertheless, in the current study, it is shown that for all of the investigated thicknesses, smaller radii can be used in the V-bending of aluminum EN AW 5083-H321 alloys.

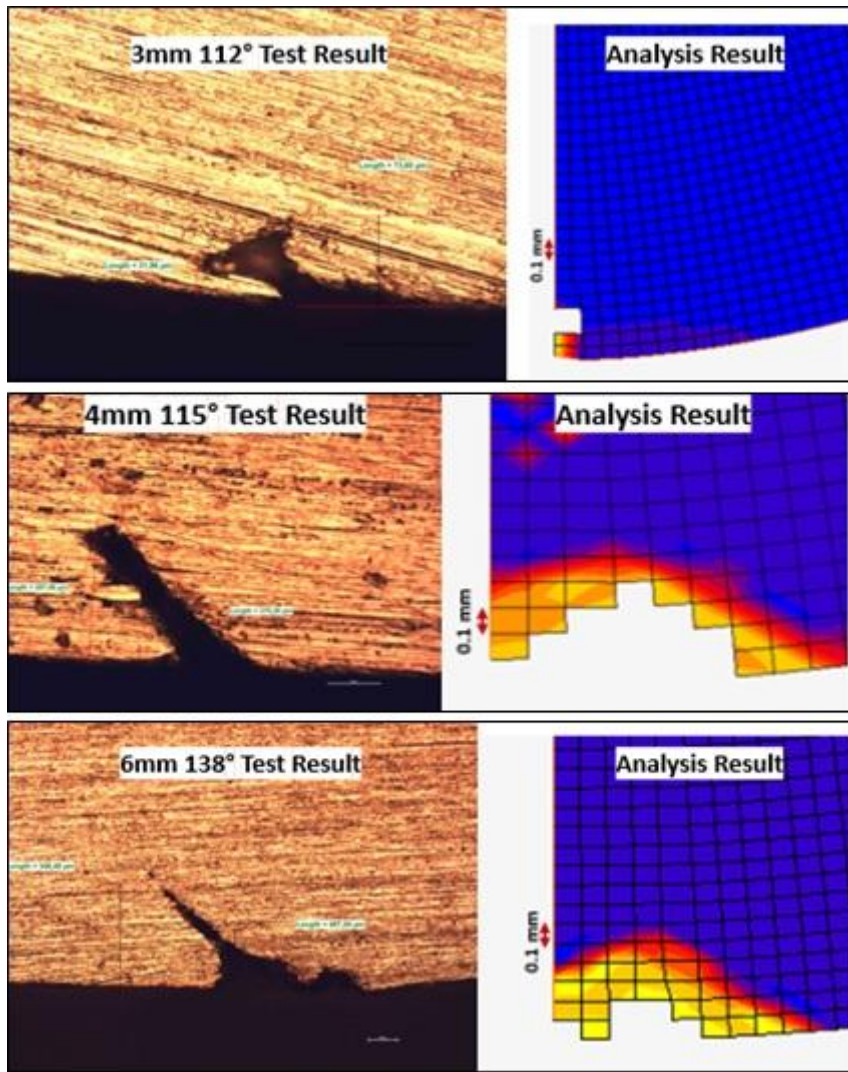


Figure 4. Bending tests and their corresponding finite element results corresponding to (top) 3 mm, (middle) 4 mm, and (bottom) 6 mm thickness aluminum sheets

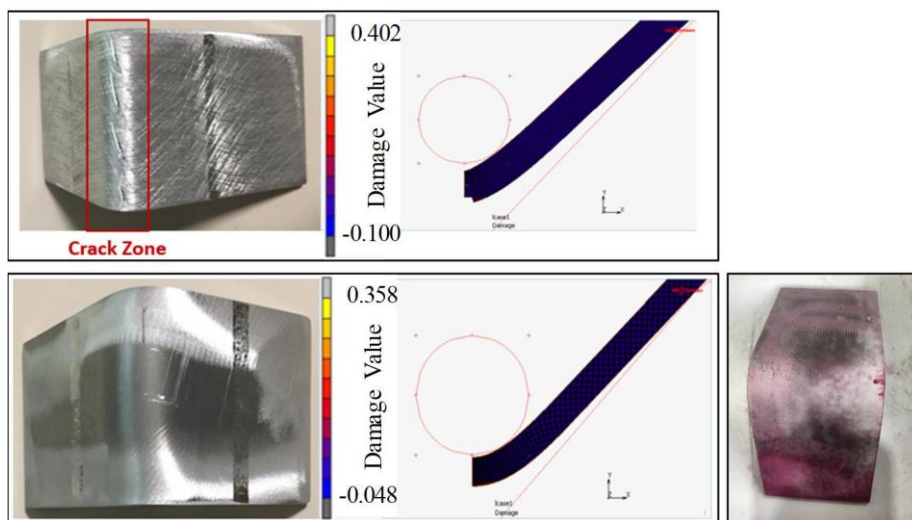


Figure 5. Bending tests and their corresponding finite element results of sheet with 3 mm thickness using (top) 4 mm bending radius and (bottom) 6 mm bending radius

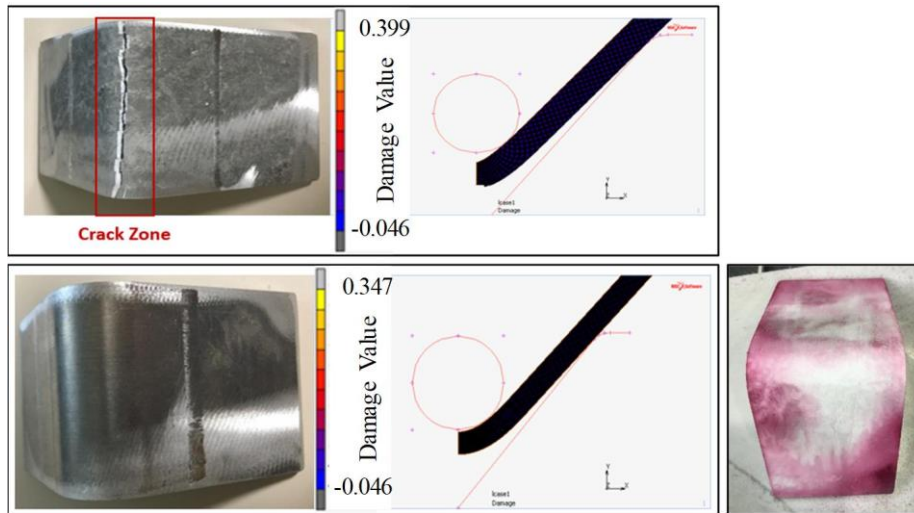


Figure 6. Bending tests and their corresponding finite element results of sheet with 4 mm thickness using (top) 6 mm bending radius and (bottom) 8 mm bending radius

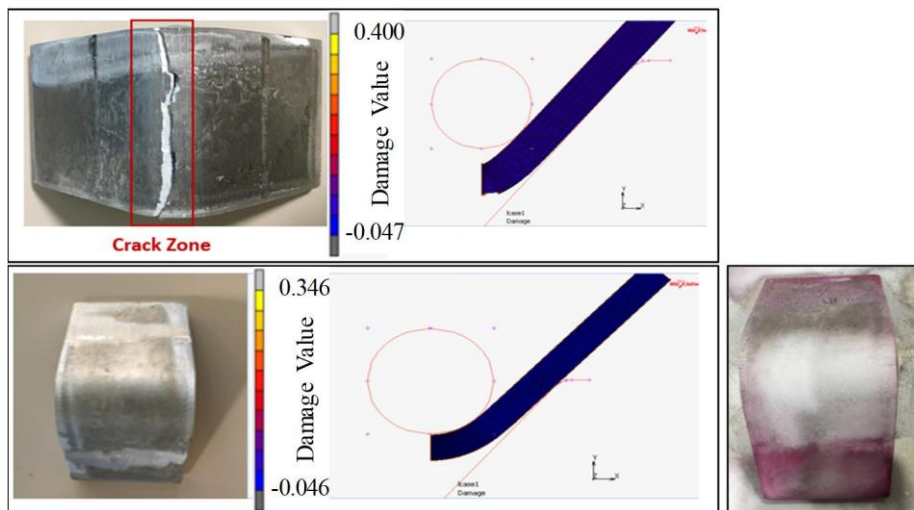


Figure 7. Bending tests and their corresponding finite element results of sheet with 6 mm thickness using (top) 8 mm bending radius and (bottom) 12 mm bending radius

4. Conclusions

Within the scope of this study, bending characteristics and fracture formation in EN AW 5083-H321 aluminum alloys are investigated using experiments and finite element analysis. Following conclusions are made:

- Bending of EN AW 5083-H321 aluminum alloy is realized under different bending radii.
- For the investigated cases, it is observed that fracture free bendings can be generated using lower radii than suggested in the corresponding standards.
- Fracture formation during the bending of EN AW 5083-H321 alloy can be modeled using finite element analysis.
- Cockroft-Latham fracture model with adjusted fracture parameters is capable of representing the fracture formation in bending process of EN AW 5083-H321 alloy.

Acknowledgements

Authors of this work thank to Scientific and Technological Research Council of Turkey for financial support under the project 217M962.

Declaration of Competing Interest

No conflict of interest was declared by the authors.

Authorship Contribution Statement

Mehmet Okan Görtan: Writing, Reviewing and Editing, Methodology, Supervision

Mehmet Ali Çiftçi: Data Preparation

References

- [1] M. Kolar, K.O. Pedersen, S. Gulbrandsen-Dahl, K. Marthinsen, “Combined effect of deformation and artificial aging on mechanical properties of Al-Mg-Si alloy,” *Trans. Nonferrous Met. Soc. China*, vol. 22, pp. 1824-1830, Aug. 2012, doi: 10.1016/S1003-6326(11)61393-9.
- [2] A. Cuniberti, A. Tolley, M.V. Castro Riglos, R. Giovachini, “Influence of natural aging on the precipitation hardening of an AlMgSi alloy,” *Mater. Sci. Eng. A*, vol. 527, pp. 5307-5311, Jul. 2010, doi: 10.1016/j.msea.2010.05.003.
- [3] H. Demir, S. Gündüz, “The effect of aging on machinability of 6061 aluminum alloy,” *Mater. Des.*, vol. 30, pp. 1480-1483, May 2009, doi: 10.1016/j.matdes.2008.08.007.
- [4] W. F. Hosford, R. M. Caddell, “*Metal Forming Mechanics and Metallurgy*”. Cambridge University Press, 3rd edition, 2007.
- [5] Standard Test Methods for Tension Testing of Metallic Materials, ASTM E8/E8M-22, 2024.
- [6] H. Kim, S. Chatti, N. Kardes, “Bending, Flanging, and Hemming” in *Sheet Metal Forming: Processes and Applications*, T. Altan, A.E. Tekkaya, Eds. Materials Park, Ohio, USA, ASM International, 2012, pp. 19-49.
- [7] Y. Huang, H. B. Wang, and F. Guo, “The improved Irwin’s model for crack problems in power-law hardening materials,” *Int. J. Appl. Mech.*, May 2023, doi: 10.1142/s1758825123500643.
- [8] X. R. Chu, L. Leotoing, D. Guines, and J. Gao, “Comparison of Constitutive Laws on the Modeling of Thermo-Viscoplastic Behaviour of an Aluminum Alloy,” *J. Appl. Mech. Mater.*, pp. 307–310, Jan. 2014, doi: 10.4028/www.scientific.net/amm.496-500.307.
- [9] J. P. Pascon, M. A. S. Torres, and C. A. R. P. Baptista, “Numerical model for the stress field ahead of a crack in elastoplastic regime,” *Procedia Struct. Integr.*, vol. 17, pp. 411–418, Jan. 2019, doi: 10.1016/J.PROSTR.2019.08.054.
- [10] H. Palaniswamy, “Plastic Deformation – State of Stress, Yield Criteria Flow Rule, and Hardening Rules,” in *Sheet Metal Forming: Fundamentals*, T. Altan, A.E. Tekkaya, Eds. Materials Park, Ohio, USA, ASM International, 2012, pp. 53-72.
- [11] K. Anoukou, F. Pastor, P. Dufrenoy, and D. Kondo, “Limit analysis and homogenization of porous materials with Mohr–Coulomb matrix. Part I: Theoretical formulation,” *J. Mech. Phys. Solids*, vol. 91, pp. 145–171, Jun. 2016, doi: 10.1016/J.JMPS.2016.01.018.
- [12] N. Kugalur-Palanisamy, E. Rivière-Lorphèvre, P.-J. Arrazola, and F. Ducobu, “Comparison of Johnson-Cook and modified Johnson-Cook material constitutive models and their influence on finite element modelling of Ti6Al4V orthogonal cutting process,” *AIP Conference Proceedings*, vol. 2113, no.1, p. 080009, Jul. 2019, doi: 10.1063/1.5112617.
- [13] P. G. Kossakowski, “Prediction of Ductile Fracture for S235JR Steel Using the Stress Modified Critical Strain and Gurson-Tvergaard-Needleman Models,” *J. Mater. Civ. Eng.*, vol. 24, no. 12, pp. 1492–1500, Dec. 2012, doi: 10.1061/(ASCE)MT.1943-5533.0000546.
- [14] Lyamina, E., Alexandrov, S., Jeng, Y.-R., & Hwang, Y. M., “Modelling of Damage Evolution in the Vicinity of Frictional Interfaces in Metal Forming,” *Adv. Mater. Res.*, Vol. 579, pp. 124–133, Oct. 2012, doi: 10.4028/WWW.SCIENTIFIC.NET/AMR.579.124.
- [15] J. K. Holmen, L. E. B. Dæhli, O. S. Hopperstad, and T. Børvik, “Prediction of ductile failure using a phenomenological model calibrated from micromechanical simulations,” *Procedia Struct. Integr.*, vol. 2, pp. 2543–2549, Dec. 2016, doi:10.1016/j.prostr.2016.06.318.
- [16] S. Alexandrov and D. Vilotic, “A theoretical—experimental method for the identification of the modified Cockcroft—Latham ductile fracture criterion,” *P. I. Mech. Eng. C-J Mec.*, vol. 222, no. 9, pp. 1869–1872, Sep. 2008, doi: 10.1243/09544062JMES1055.
- [17] *Aluminium and Aluminium Alloys – Chemical Composition and Form of Wrought Products*, DIN EN 573-3, 2022.
- [18] *Aluminium and Aluminium Alloys – Sheet, Strip and Plate*, DIN EN 00485-2, 2007.